

# Evolution of the Fermi surface of $\text{BaFe}_2(\text{As}_{1-x}\text{P}_x)_2$ on entering the superconducting dome

H. Shishido,<sup>1,2</sup> A.F. Bangura,<sup>3</sup> A.I. Coldea,<sup>3</sup> S. Tonegawa,<sup>1</sup> K. Hashimoto,<sup>1</sup> S. Kasahara,<sup>2</sup> P.M.C. Rourke,<sup>3</sup> H. Ikeda,<sup>1</sup> T. Terashima,<sup>2</sup> R. Settai,<sup>4</sup> Y. Ōnuki,<sup>4</sup> D. Vignolles,<sup>5</sup> C. Proust,<sup>5</sup> B. Vignolle,<sup>5</sup> A. McCollam,<sup>6</sup> Y. Matsuda,<sup>1</sup> T. Shibauchi,<sup>1</sup> and A. Carrington<sup>3</sup>

<sup>1</sup>*Department of Physics, Kyoto University, Sakyo-ku, Kyoto 606-8502, Japan.*

<sup>2</sup>*Research Center for Low Temperature and Materials Sciences, Kyoto University, Sakyo-ku, Kyoto 606-8501, Japan.*

<sup>3</sup>*H. H. Wills Physics Laboratory, Bristol University, Tyndall Avenue, BS8 1TL, United Kingdom.*

<sup>4</sup>*Graduate School of Science, Osaka University, Toyonaka, Osaka 560-0043, Japan.*

<sup>5</sup>*Laboratoire National des Champs Magnétiques Intenses (CNRS), Toulouse, France.*

<sup>6</sup>*High Field Magnet Laboratory, Institute for Molecules and Materials, Radboud University Nijmegen, Toernooiveld 7, 6525 ED Nijmegen, The Netherlands*

Using the de Haas-van Alphen effect we have measured the evolution of the Fermi surface of  $\text{BaFe}_2(\text{As}_{1-x}\text{P}_x)_2$  as function of isoelectric substitution (As/P) for  $0.41 < x < 1$  ( $T_c$  up to 25 K). We find that the volume of electron and hole Fermi surfaces shrink linearly with decreasing  $x$ . This shrinking is accompanied by a strong increase in the quasiparticle effective mass as  $x$  is tuned toward the maximum  $T_c$ . It is likely that these trends originate from the many-body interaction which gives rise to superconductivity, rather than the underlying one-electron bandstructure.

Superconductivity in the 122 iron-pnictide family  $\text{XFe}_2\text{As}_2$  (where X=Ba,Sr or Ca), can be induced by a variety of means, including doping [1, 2], pressure [3] or isoelectric substitution either on the Fe [4] or As sites [5]. The highest  $T_c$  achievable by each of these routes is roughly the same. It has been suggested [6, 7, 8] that the interband coupling between the hole and electron sheets plays an important role in determining the magnetic or superconducting order formed at low temperature. Discovering how the Fermi surface evolves as a function of the various material parameters which drive the material from an antiferromagnetic spin density wave state, through the superconducting dome and eventually towards a paramagnetic non-superconducting metal, should therefore be an important step toward gaining a complete understanding of the mechanism that drives high temperature superconductivity in these materials.

In the antiferromagnetic state it is expected that the Fermi surface suffers a major reconstruction. This is supported experimentally by the observation [9, 10, 11] of very low frequency quantum oscillations in the undoped  $\text{XFe}_2\text{As}_2$  compounds, corresponding to very small Fermi surface pockets which are 1-2% of the total Brillouin zone planar area. At the other extreme of the phase diagram, where the materials are paramagnetic and non-superconducting, quantum oscillation measurements of  $\text{SrFe}_2\text{P}_2$  [12] and  $\text{CaFe}_2\text{P}_2$  [13] show that the Fermi surface is in good agreement with conventional bandstructure calculations. Up to now, tracking the changes in the Fermi surface across the phase diagram using quantum oscillations has not been possible because of the additional disorder and high  $H_{c2}$  introduced by doping. Measurements on the low  $T_c$  (6 K) superconducting iron-pnictide  $\text{LaFePO}$  [14, 15] established that the Fermi surface is in broad agreement with bandstructure with mod-

erate correlation enhancements of the effective mass. It is not clear whether the higher  $T_c$  pnictide superconductors, which unlike  $\text{LaFePO}$  occur in close proximity to a magnetic phase, are also well described by bandstructure and whether the electronic correlations change significantly.

The substitution of P for As in the series  $\text{BaFe}_2(\text{As}_{1-x}\text{P}_x)_2$  offers an elegant way to suppress magnetism and induce superconductivity without doping [16]. As P and As are isoelectric, there is no net change in the ratio of electrons to holes and the system remains a compensated metal for different  $x$  (equal volumes for the electron and hole Fermi surfaces). This series has several remarkable properties which are similar to those observed in cuprate superconductors. Firstly, the temperature dependence of the resistivity changes from a quadratic ( $\rho \sim T^2$ ) to linear behavior ( $\rho \sim T$ ) as the system evolves from a conventional Fermi liquid ( $x = 1$ ) towards the maximum  $T_c$  ( $x = 0.33$ ). Secondly, there is strong evidence from magnetic penetration depth [17], thermal conductivity [17] and NMR [18] measurements that for  $x = 0.33$  the superconducting gap has line nodes.

In this Letter, we report the observation of quantum oscillation signals in samples of  $\text{BaFe}_2(\text{As}_{1-x}\text{P}_x)_2$  as  $x$  is varied across the superconducting dome from  $x = 1$  to  $x = 0.41$  with  $T_c \sim 25$  K ( $\simeq 0.8 T_c^{\text{max}}$ ). Our data show that the Fermi surface shrinks and the quasiparticle masses become heavier as the material is tuned toward the magnetic order phase boundary, at which  $T_c$  reaches its maximum. This implies that the significant change of electronic structure caused by many-body interactions plays a key role for the occurrence of unconventional high- $T_c$  superconductivity.

Single crystal samples of  $\text{BaFe}_2(\text{As}_{1-x}\text{P}_x)_2$  were grown as described in Ref. [16]. The  $x$  values were determined by an energy dispersive X-ray analyzer. Measurements of

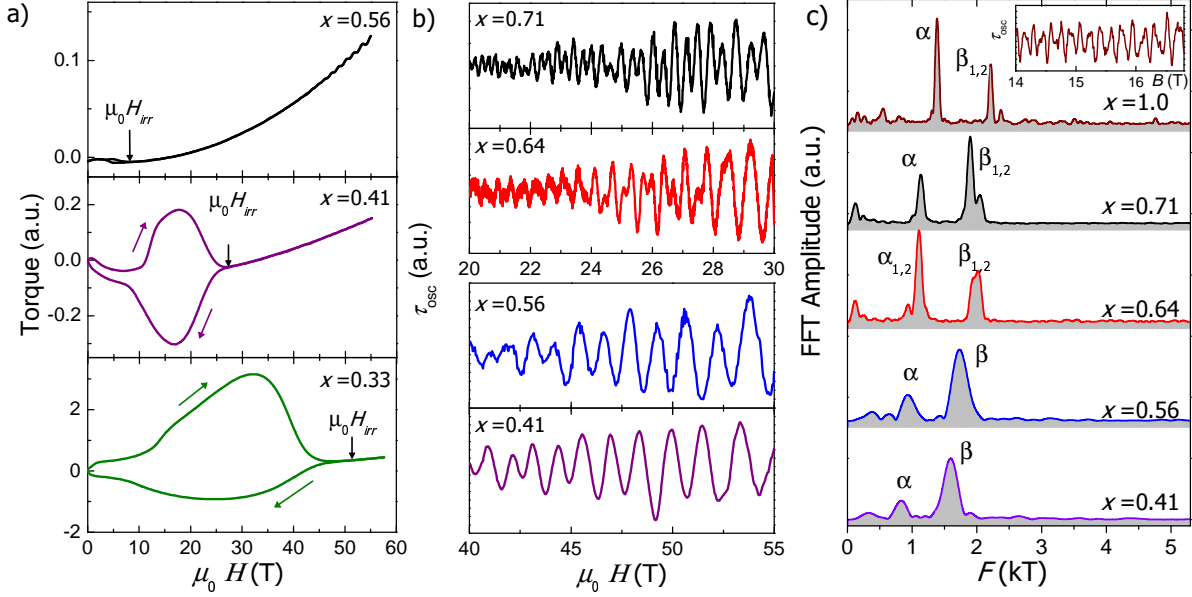


FIG. 1: (color online). a) Raw torque data for  $\text{BaFe}_2(\text{As}_{1-x}\text{P}_x)_2$  with  $x = 0.33, 0.41, 0.56$  measured at 1.5 K. b) The oscillatory part of torque for selected samples and c) the corresponding Fourier transform for  $x = 0.41, 0.56$  between 35-55 T at 1.5 K and  $x = 0.64, 0.71$  between 20-30 T at 0.35 K as well as  $x = 1$  between 12-16.8 T at 0.092 K. The inset shows the oscillatory signal for  $x = 1.0$ .

the quantum oscillations in magnetic torque [the de Haas-van Alphen (dHvA) effect] were made using a miniature piezo-resistive cantilever technique. Experiments were performed in: a dilution refrigerator system with DC fields up to 17 T (Osaka), a pumped  $^3\text{He}$  system with DC fields up to 30 T (Nijmegen) and 45 T (Tallahassee) and a pumped  $^4\text{He}$  system with pulsed fields up to 55 T (Toulouse). Our data are compared to band structure calculations which were performed using the WIEN2K package [19].

Fig. 1(a) shows raw magnetotorque  $\tau(H)$  data for three values of  $x$  measured up to 55 T at  $T \simeq 1.5$  K, with the magnetic field direction close to the  $c$ -axis. The torque response for the higher  $T_c$  samples ( $x = 0.33$ ,  $T_c \simeq 30$  K and  $x = 0.41$ ,  $T_c \simeq 25$  K) is highly hysteretic.  $\mu_0 H_{irr}$  increased substantially with  $x$  reaching a maximum of 51.5 T for the highest  $T_c$  sample ( $x = 0.33$ ), which is close to the estimated  $H_{c2}$  value [17]. By subtracting a smooth polynomial background the oscillatory dHvA signal is clearly seen above  $H_{irr}$  (Fig. 1(b)) for all samples except for that with the highest  $T_c$  ( $x = 0.33$ ).

From the fast Fourier transform (FFT) spectra of the oscillatory data (Fig. 1(c)) we can extract the dHvA frequencies  $F$ . These are related to the extremal cross-sectional areas,  $A_k$ , of the Fermi surface orbits giving rise to the oscillations via the Onsager relation,  $F = (\hbar/2\pi e)A_k$ . From the evolution of these frequencies (see Fig. 2) as the magnetic field is rotated from being along the  $c$  axis ( $\theta = 0^\circ$ ) towards being perpendicular the  $c$  axis ( $\theta = 90^\circ$ ), we can deduce the shape of the Fermi

surface.

Band structure calculations of the Fermi surface of the end members of the  $\text{BaFe}_2(\text{As}_{1-x}\text{P}_x)_2$  series are shown in Fig. 2. For both  $\text{BaFe}_2\text{As}_2$  and  $\text{BaFe}_2\text{P}_2$  the calculations were done with the experimental lattice parameters and pnictide  $z$  position in the non-magnetic state. The two electron sheets at the zone corner are quite similar in size and shape in both compounds but there are significant differences between the hole sheets. In  $\text{BaFe}_2\text{As}_2$  three concentric quasi-two-dimensional hole tubes are located at the zone center, whereas in  $\text{BaFe}_2\text{P}_2$  the inner one of these tubes is absent whereas the outer tube has become extremely warped. The Fermi surface of  $\text{BaFe}_2\text{P}_2$  is quite similar to that for  $\text{SrFe}_2\text{P}_2$  [12].

For  $\text{SrFe}_2\text{P}_2$  [12],  $\text{CaFe}_2\text{P}_2$  [13] and  $\text{LaFePO}$  [14] it was observed that the strongest dHvA signals came from the electron sheets and so this is likely also to be the case for  $\text{BaFe}_2\text{P}_2$ . Thus, we assign the two strongest peaks ( $\alpha$  and  $\beta$ ) to the inner and outer electron sheet, respectively (see Fig. 1(c)). The observed frequencies for  $x = 1$  are somewhat smaller than those predicted by the calculations and a rigid band shift of 45 – 75 meV is needed to bring the orbits into agreement with experiment. This is quite comparable to the shifts 50 – 60 meV needed for the electron sheets in  $\text{SrFe}_2\text{P}_2$  [12]. Although there are other weak peaks in the FFT which could come from the hole sheets, further measurements with better signal to noise ratio are needed to confirm these.

As the sample composition is varied towards optimal doping, the signal from the electron sheets is reduced but

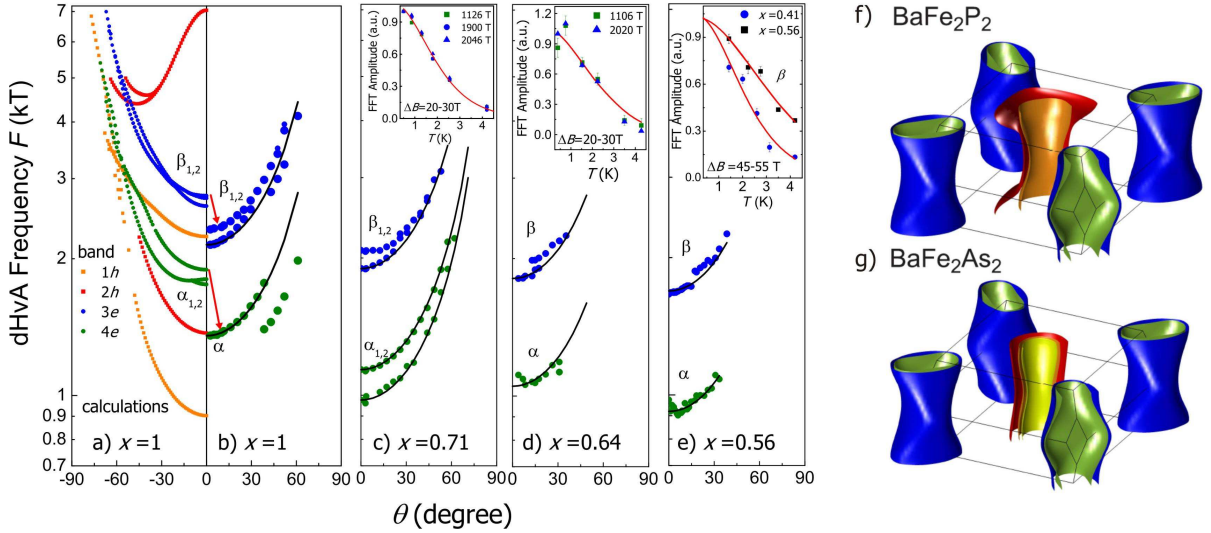


FIG. 2: (color online). a) Angle dependence of the predicted orbits from  $B \parallel [001]$  ( $\theta = 0^\circ$ ) to  $B \parallel [100]$  ( $\theta = 90^\circ$ ) for  $x = 1$  (BaFe<sub>2</sub>P<sub>2</sub>) and the electron orbits observed experimentally for b)  $x = 1$ , c)  $x = 0.72$ , d)  $x = 0.64$ , e)  $x = 0.56$ . Solid lines correspond to  $F(\theta = 0)/\cos \theta$ . The insets show the temperature dependence of the Fourier amplitudes for each composition, which are fitted (solid line) to the Lifshitz-Kosevich formula  $X/\sinh X$ ,  $X = 14.69 m^* T/B$  to determine the effective masses,  $m^*$  [20]. The calculated Fermi surfaces of the end members, f) BaFe<sub>2</sub>As<sub>2</sub> (non-magnetic) and g) BaFe<sub>2</sub>P<sub>2</sub> are also shown.

two peaks are clearly visible over the full doping range in sufficiently high fields (see Fig. 1(c)); the mean free path for the  $\beta$  orbits decreases from  $\ell \sim 800 \text{ \AA}$  to  $170 \text{ \AA}$  when  $x$  varies from  $x = 1$  to  $0.41$ . Importantly, we observe that the frequency of both these electron orbits decreases linearly with decreasing  $x$  (see Fig. 3(a)). For  $x = 1$  the  $\beta$  frequency equals  $2.30 \text{ kT}$  which decreases to  $1.55 \text{ kT}$  for  $x = 0.41$ . Although we do not clearly observe them, charge neutrality means that the hole sheets must shrink by the same factor.

The effective masses of the quasiparticles on the various orbits were determined by fitting the temperature dependent amplitude of the oscillations to the Lifshitz-Kosevich formula [20] (see insets of Fig. 2). As shown in Fig. 3(b), the effective mass increases significantly as  $x$  approaches the spin density wave ordered phase. At the same time  $T_c$  increases and shows a maximum at the boundary of the magnetic order. As no such increase is expected from the bandstructure (see later) the result implies a significant rise in the strength of the many-body interactions, most likely caused by spin-fluctuations. A similar striking rise in the mass enhancement close to an antiferromagnetic quantum critical point has also been observed in quasi-two dimensional heavy-Fermion systems [21].

For  $x = 1$  bare masses calculated from the bandstructure for the electron sheets vary from  $0.8$  to  $1.0 m_e$ . To obtain a dHvA frequency of  $1.55 \text{ kT}$ , appropriate for  $x = 0.41$ , requires a rigid shift of the energy of band 4 (see Fig. 2(a)) by  $170 \text{ meV}$ . The bare mass then decreases from  $0.92$  to  $0.81 m_e$ , in sharp contrast to the large rise seen in experiment. The many body enhancement factor

$m^*/m_b$  therefore increases from  $\sim 2$  to  $\sim 4$  as  $x$  decreases from  $1$  to  $0.41$ . Note that conventional electron-phonon coupling is weak in these materials, and is estimated to only account for  $\sim 25\%$  of the observed mass enhancement [22].

The shrinking of the electron and hole sheets as  $x$  decreases could come from either the underlying one-electron bandstructure or alternatively it could be driven by many-body correlation effects. We have estimated the change in the electron sheet area by calculating the bandstructure for both BaFe<sub>2</sub>As<sub>2</sub> and BaFe<sub>2</sub>P<sub>2</sub> with values of the lattice constants and  $z$  fixed to the experimental values appropriate for the various values of  $x$ . Experimentally it is found that these parameters follow Vegard's law and scale linearly with  $x$  [16]. We find that for both the As and P material the  $\alpha$  and  $\beta$  frequencies vary relatively little with  $x$ . In Fig. 3(a) we show a weighted average of these calculated frequencies,  $F_{av} = xF_P + (1-x)F_{As}$  where  $F_P/F_{As}$  refers to the (average maximal and minimal extremal) frequencies calculated with the atom set to P or As respectively. The calculated changes are much smaller than we observe experimentally, so it seems unlikely that the shrinking electron sheets can be explained by conventional bandstructure theory.

An alternative is that the shrinking is driven by many-body effects. Recently, Ortenzi *et al.* [23] suggested that in LaFePO the shrinking of the electron and hole Fermi-surfaces and enhancement of effective masses can be explained by the interaction between the electron and hole bands. The observed correlation of the Fermi surface areas with the increase in effective mass and increase in  $T_c$  would be consistent with this model; however, it remains

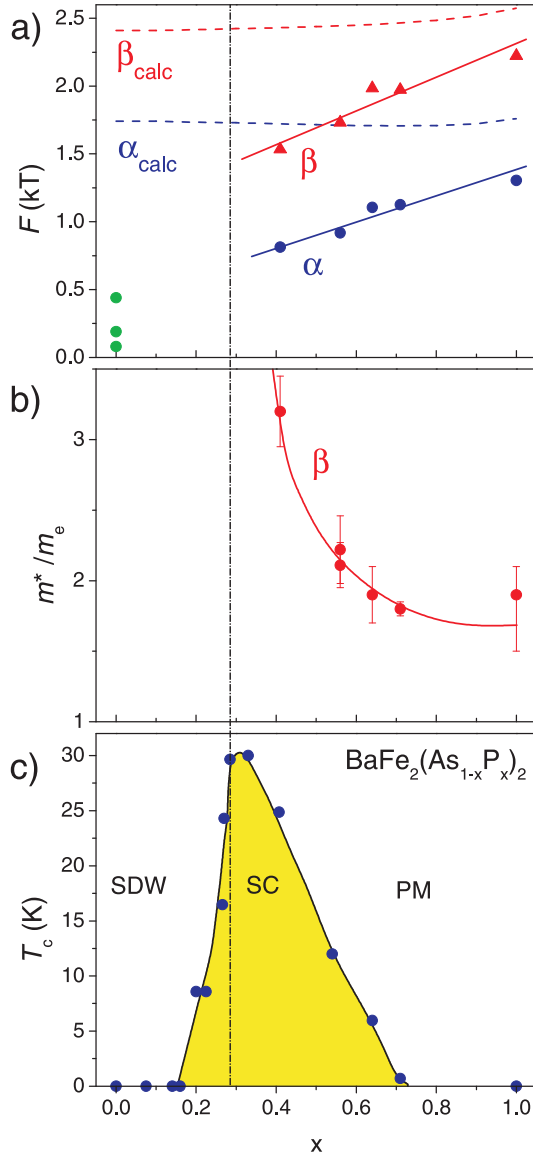


FIG. 3: color online. (a) Experimental (solid symbols) average electron sheet frequencies ( $\alpha$  and  $\beta$ ) versus P content,  $x$ . The data for  $x = 0$  are taken from Ref. [9]. The dashed lines show bandstructure predictions. (b) The variation with  $x$  of the quasiparticle effective masses,  $m^*$  and (c)  $T_c$  after Ref. [16]. The vertical dashed line marks the location of the onset of the appearance of magnetism at  $T = 0$ .

to be seen if quantitative agreement can be achieved.

In summary, we have presented dHvA data which shows the evolution of the Fermi surface of  $\text{BaFe}_2(\text{As}_{1-x}\text{P}_x)_2$  as  $x$  is varied towards  $T_c^{\text{max}}$ . We find that the volume of the electron sheets (and via charge neutrality also the hole sheets) shrink linearly and the effective masses become strongly enhanced with decreasing  $x$ . It seems unlikely that these changes are a simple consequence of the one-electron bandstructure but instead they likely originate from many-body interactions. These changes may be intimately related

to the high  $T_c$  unconventional superconductivity in this system.

We thank J. Analytis for helpful discussions and E.A. Yelland for the use of computer code. Part of this work has been done with the financial support of the UK's EPSRC and Royal Society, EuroMagNET under the EU contract no.228043, Scientific Research on Priority Areas of New Materials Science Using Regulated Nano Spaces (20045008), Grant-in-Aid for Scientific Research on Innovative Areas "Heavy Electrons (20102002), Specially Promoted Research (2001004) and Grant-in-Aid for GCOE program 'The Next Generation of Physics, Spun from Universality and Emergence' from MEXT, Japan. Work performed at the NHMFL in Tallahassee, Florida, was supported by NSF Cooperative Agreement No. DMR-0654118, by the State of Florida, and by the DOE.

- 
- [1] M. Rotter, M. Tegel, and D. Johrendt, Phys. Rev. Lett. **101**, 107006 (2008).
  - [2] A. S. Sefat, *et al.*, Phys. Rev. Lett. **101**, 117004 (2008).
  - [3] P. Alireza, *et al.*, J. Phys. Cond. Mat. **21**, 012208 (2008).
  - [4] S. Paulraj, *et al.*, arXiv: 0902.2728.
  - [5] S. Jiang, *et al.*, J. Phys. Cond. Mat. **21**, 382203 (2009).
  - [6] K. Kuroki, H. Usui, S. Onari, R. Arita, and H. Aoki, Phys. Rev. B **79**, 224511 (2009).
  - [7] A. V. Chubukov, D. V. Efremov, and I. Eremin, Phys. Rev. B **78**, 134512 (2008).
  - [8] I. I. Mazin, D. J. Singh, M. D. Johannes, and M. H. Du, Phys. Rev. Lett. **101**, 057003 (2008).
  - [9] J. G. Analytis, *et al.*, Phys. Rev. B **80**, 064507 (2009).
  - [10] N. Harrison, *et al.*, J. Phys. Cond. Mat. **21**, 322202 (2009).
  - [11] S. E. Sebastian, *et al.*, J. Phys. Cond. Mat. **20**, 422203 (2008).
  - [12] J. G. Analytis, *et al.*, Phys. Rev. Lett. **103**, 076401 (2009).
  - [13] A. I. Coldea, *et al.*, Phys. Rev. Lett. **103**, 026404 (2009).
  - [14] A. I. Coldea, *et al.*, Phys. Rev. Lett. **101**, 216402 (2008).
  - [15] H. Sugawara, *et al.*, J. Phys. Soc. Jap. **77**, 113711 (2008).
  - [16] S. Kasahara, *et al.*, arXiv:0905.4427.
  - [17] K. Hashimoto, *et al.*, arXiv:0907.4399.
  - [18] Y. Nakai, *et al.*, arXiv:0908.0625.
  - [19] P. Blaha, K. Schwarz, G. K. H. Madsen, D. Kvasnicka, and J. Luitz, *WIEN2K, An Augmented Plane Wave + Local Orbitals Program for Calculating Crystal Properties* (Karlheinz Schwarz, Techn. Universität Wien, Austria, 2001).
  - [20] D. Schoenberg, Magnetic Oscillations in Metals *Cambridge University Press*, London, 1984.
  - [21] H. Shishido, R. Settai, H. Harima, and Y. Onuki, J. Phys. Soc. Jpn. **74**, 1103 (2005).
  - [22] T. Yildirim, Phys. Rev. Lett. **102**, 037003 (2009).
  - [23] L. Ortenzi, E. Cappelluti, L. Benfatto, and L. Pietronero, Phys. Rev. Lett. **103**, 046404 (2009).